Spontaneous photon emission in isolated-core excited Rydberg systems and dynamics of electronic wave packets

O. Zobay and G. Alber

Theoretische Quantendynamik, Fakultät für Physik, Universität Freiburg, D-79104 Freiburg im Breisgau, Germany

In isolated-core excited Rydberg systems the destruction of quantum coherence by spontaneous emission of photons is investigated. For this purpose a theoretical description is developed which is based on a decomposition of the atomic density operator into N-photon contributions. Using methods from multichannel quantum defect theory, the relevant atomic transition amplitudes are represented in the form of semiclassical path representations which are associated with repeated returns of the Rydberg electron to the ionic core. Apart from numerical advantages, this approach also yields a clear physical picture of the intricate interplay between the incoherent photon emission process, the coherent laser-modified electron correlation effects, and the semiclassical aspects of the dynamics of the Rydberg electron. Various examples of this interplay are analyzed within the framework of the developed theoretical tools. [S1050-2947(96)04012-7]

I. INTRODUCTION

Electronic Rydberg wave packets are physical objects which are situated on the border between microscopic and macroscopic physics. This implies that their dynamical behavior shows an interesting interplay between classical and quantum mechanical aspects. During the past decade, much effort on both the theoretical and the experimental side has successfully been invested to shed some light onto this interplay in various contexts [1]. In particular, attention was drawn recently to the study of wave packet dynamics in isolated-core excited atoms in which the near-classical Rydberg electron interacts with a purely quantum mechanical object, namely, a Rabi-oscillating two-level atomic core. This system was shown to display new interesting dynamical properties [2,3].

In isolated-core excitation (ICE) processes [4] which provide the basis for these studies, initially an outer valence electron is excited to a Rydberg state with one or several laser pulses. Subsequently, transitions in the positively charged ionic core are induced with the help of a second laser. Thereby the Rydberg electron essentially plays the role of a spectator and is affected by the core transition only through the process of shakeup, which leads to a change of its principal quantum number. This shakeup is made possible by a difference in the quantum defects of the two Rydberg series involved in the transition. Perturbative isolated-core excitation processes with a weak laser field driving the core transition nowadays provide a well-established tool in frequency-resolved studies of highly excited Rydberg states in two-electron-like atoms [5] and have also been used as a means of preparing autoionizing wave packets [6,7]. Nonperturbative effects due to ICE or related processes and induced by a short and strong laser pulse have been investigated by various groups experimentally in the recent past [8–11]. Similar studies for an intense continuous-wave laser field have been performed theoretically in both the energy-resolved [12–15] and the time-resolved domain [2,3].

In the context of wave packet dynamics in Rydberg sys-

tems the study of dissipative and stochastic influences which destroy quantum coherences has not received much attention so far. This might be attributed to the fact that in general in systems with a large number of relevant states, as in Rydberg systems, the solution of the appropriate master equations constitutes a difficult mathematical and numerical problem. Such studies, however, would be important from both a fundamental and a pragmatic point of view. Motivated by recent investigations on ICE wave packet dynamics [2,3] in this article the influence of spontaneous decay processes of a laser-excited core on an electronic Rydberg wave packet is investigated. The purpose of the presentation is twofold: (1) to obtain physical insight into the intricate interplay between laser-modified electron correlation effects, which take place inside the core region, the spontaneous emission of photons by the core, which is of a stochastic nature and tends to destroy quantum coherence, and the semiclassical aspects of the dynamics of the excited Rydberg electron and (2) to develop an adequate theoretical approach to this problem, which is capable of dealing with the difficulties associated with the description of dissipative phenomena in Rydberg systems close to a photoionization threshold.

Our theoretical approach is based on the combination of two efficient theoretical tools, namely, Mollow's pure state analysis of resonance fluorescence [16] and multichannel quantum defect theory (MQDT) [17]. According to Mollow's approach to resonance fluorescence the solution of a master equation for the reduced atomic density operator, which describes the decay of coherence due to spontaneous emission of photons, can be obtained by averaging over an ensemble of pure atomic states each of which is characterized by the number of spontaneously emitted photons N and the associated random photon emission times $t_1 \leq \cdots \leq t_N$. This pure state approach, which is also the theoretical basis for recently developed quantum Monte Carlo wave function approaches to dissipation [18–20], is expected to offer significant advantages over a direct solution of a master equation, in particular, in cases in which an electronic Rydberg wave packet is prepared close to a threshold and the number

of relevant atomic states is large or even infinite. Whereas Mollow's approach allows one to express the solution of a master equation in terms of pure states, MQDT is a powerful theoretical tool for dealing with threshold phenomena arising from the presence of infinite many Rydberg and continuum states. Thus the combination of these two theoretical methods is expected to offer significant advantages in the treatment of dissipative phenomena in Rydberg systems. Furthermore, with the help of MQDT semiclassical path representations can be derived for relevant atomic transition amplitudes which clearly exhibit the intricate relation between coherent laser-modified electron correlation effects, the incoherent spontaneous emission of photons by the core, and the semiclassical aspects of the dynamics of the excited Rydberg electron in a quantitative and qualitative way. Though in the following our discussion will concentrate on Rydberg atoms, the theoretical methods developed are expected to be applicable to dissipative phenomena of any kind which affect the dynamics of a Rydberg electron only indirectly through the ionic core and which can be described by a master equation for the reduced density operator of the Rydberg system. Furthermore, due to the universal properties of Rydberg systems which originate from the long-range nature of the Coulomb potential [21] most of our results are not only valid for atomic but also for molecular [22] Rydberg systems.

As to the physical applications of the presented theoretical approach, we consider in particular the influence of spontaneous emission on the effect of stabilization of a Rydberg wave packet against autoionization by synchronizing the Rabi period of the oscillating core with the orbit time of the wave packet [3]. Due to the stochastic nature of the spontaneous photon emission process, this synchronization will be disturbed as soon as a photon has been emitted by the core. The ensuing modifications of the autoionization dynamics can be well described with the help of the theoretical tools developed. The effects of spontaneous emission are shown to be of relevance in certain kinds of experiments studying the stabilization effect.

This article is organized as follows. In Sec. II the basic ideas of our theoretical approach are presented and semiclassical path representations for the relevant atomic N-photon transition amplitudes are derived. For the sake of a clear presentation our discussion will concentrate on a model three-channel problem and details of the derivation of the theoretical results are summarized in the Appendix. In Sec. III with the help of this theoretical approach characteristic physical aspects of wave packet dynamics in the presence of a spontaneously decaying core (in the absence of a core-dressing laser field) and in the presence of resonance fluorescence of the ionic core are investigated. Besides studying the interplay between autoionization and spontaneous emission we also examine the influence of dissipation on the long-time dynamics of nonautoionizing model systems.

II. RESONANCE FLUORESCENCE IN ISOLATED-CORE EXCITED RYDBERG SYSTEMS

In this section a theoretical description of electronic Rydberg wave packet dynamics in isolated-core excited Rydberg systems under the influence of resonance fluorescence
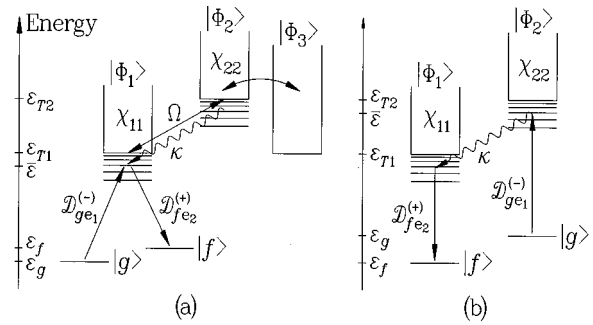

FIG. 1. Model excitation schemes: (a) three-channel system including laser-induced core coupling and autoionization, (b) two-channel system with channel coupling only through spontaneous core decay (considered in Sec. III A).

processes is developed which is based on Mollow's description of resonance fluorescence and MQDT. For the sake of clarity our discussion will concentrate on a three-channel model problem which will be introduced in Sec. II A. The corresponding pump-probe signal with which the wave packet dynamics can be monitored may be represented as a sum over contributions of subensembles each of which has undergone a specific number $N=0,1,2,\ldots$ of spontaneous emission acts. For the relevant N-photon transition amplitudes, semiclassical path expansions are derived in Sec. II B which yield a clear physical picture of the influence of the stochastic photon emission process on the semiclassical aspects of the dynamics of the Rydberg electron. For the sake of clarity, details of the derivation of these results will be presented in the Appendix.

A. Description of the model

The essential features of the problem may be investigated with the help of an excitation scheme as shown schematically in Fig. 1(a) (however, the discussion could immediately be generalized to more complicated cases). Atomic units with $e=\hbar=m_e=1$ will be used in the following. Initially the atom is prepared in an energetically low lying bound state $|g\rangle$ with energy ε_g. The atom is situated in a cw-laser field

$$\mathbf{E}(t)=\mathcal{E}\mathbf{e}e^{-i\omega t}+\text{c.c.},\qquad(1)$$

with amplitude $\mathcal{E}$ and polarization $\mathbf{e}$, which is tuned near resonance with a transition $|\Phi_1\rangle\rightarrow|\Phi_2\rangle$ of the positively charged ionic core. The field intensity I is assumed to be small compared to the atomic unit, i.e., $I\ll10^{17}$ Wcm^{-2}. Typically electron correlations imply that as long as the atom remains in the initial state $|g\rangle$ this laser field is well detuned from any atomic transition. Therefore, it has a negligible effect on the atomic dynamics. Around time $t_a=0$, a short and weak pump pulse

$$\mathbf{E}_1(t)=\mathcal{E}_1(t)\ \mathbf{e}_1e^{-i\omega_1 t}+\text{c.c.},\qquad(2)$$

with $\mathcal{E}_1(t)$ denoting the pulse envelope of width τ_1, is applied to the atom which excites Rydberg states in channel 1 close to the photoionization threshold, thus preparing a radial electronic Rydberg wave packet. As soon as the wave packet is created the ionic core starts to perform Rabi oscillations due to the presence of the cw-laser field $\mathbf{E}(t)$. Whenever the

ionic core is in the excited state $|\Phi_2\rangle$ the Rydberg state can autoionize into the (flat) continuum channel 3. In addition to stimulated processes, the excited core is also allowed to decay to its ground state $|\Phi_1\rangle$ by spontaneous emission of a photon with a decay rate of κ. The influence of this core dynamics on the dynamics of the excited electronic Rydberg wave packet can be investigated with the help of pump-probe spectroscopy by means of applying a second short and weak laser pulse (envelope $\mathcal{E}_2$, frequency ω_2, polarization $\mathbf{e}_2$, pulse duration τ_2) centered around time t_b, which induces transitions to an energetically low lying bound state $|f\rangle$. For the sake of simplicity we set $\varepsilon_g + \omega_1 = \varepsilon_f + \omega_2 = \overline{\varepsilon}$. In the following it is assumed that spontaneous emission of photons during the application of the pump and probe pulses can be neglected, i.e.,

$$\kappa \tau_{1,2} \ll 1. \tag{3}$$

In this case the pump-probe transition probability, i.e., the probability of detecting the atom after the interaction with both laser pulses in state $|f\rangle$, is given by [1]

$$P_{g \to f}(t_b - t_a) = \langle \psi_f | \rho(t_b - t_a) | \psi_f \rangle. \tag{4}$$

It gives a measure for finding the electronic wave packet at time t_b close to the nucleus and the core in state $|\Phi_1\rangle$. Thereby, the reduced density operator of the atom is denoted $\rho(t)$, and

$$|\psi_f\rangle = i\widetilde{\mathcal{E}}_2(H - \overline{\varepsilon})\mathbf{d} \cdot \mathbf{e}_2 |f\rangle \tag{5}$$

designates the atomic state onto which the density operator is projected by application of the probe pulse [23]. Similarly, the atomic state prepared by the pump pulse is given by

$$|\psi_g\rangle = i\widetilde{\mathcal{E}}_1(H - \overline{\varepsilon})\mathbf{d} \cdot \mathbf{e}_1 |g\rangle, \tag{6}$$

with $\mathbf{d}$ denoting the atomic dipole operator,

$$\widetilde{\mathcal{E}}_{1,2}(\varepsilon) = \int_{-\infty}^{\infty} dt \mathcal{E}_{1,2}(t) e^{i\varepsilon(t - t_{a,b})}$$

the Fourier transforms of the envelopes of pump and probe pulse, and H the Hamiltonian which would describe the subsequent time evolution of the electronic wave packet in the absence of spontaneous emission processes. In the numerical examples of Sec. III the envelope function is chosen to be of the form $\mathcal{E}_{1(2)}(t) = \mathcal{E}_{1(2)}^{(0)} \exp[-4 (\ln 2)(t - t_{a(b)})^2/\tau^2]$.

The main problem is thus the evaluation of the reduced density operator of the atom $\rho(t)$ (in which the unobserved, initially unoccupied modes of the radiation field have been traced out) describing the dynamics of the Rydberg system under the stochastic influence of the photon emission process. This density operator obeys an optical Bloch equation [16]

$$\dot{\rho}(t) = -i[H, \rho(t)] + \tfrac{1}{2}\{[L, \rho(t)L^{\dagger}] + [L\rho(t), L^{\dagger}]\}. \tag{7}$$

The deterministic part of the atomic dynamics is described by the Hamiltonian

$$H = H_A + V_{\text{ICE}}, \tag{8}$$

with

$$H_A = \sum_{j=1}^{3} \{[\mathbf{h}_{jj} + \mathbf{V}_{jj}(r) + \varepsilon_{cj}]|\Phi_j\rangle\langle\Phi_j|\}$$
$$+ \mathbf{V}_{23}(r)(|\Phi_3\rangle\langle\Phi_2| + |\Phi_2\rangle\langle\Phi_3|) \tag{9}$$

and

$$V_{\text{ICE}} = -\tfrac{1}{2}\Omega(|\Phi_2\rangle\langle\Phi_1| + |\Phi_1\rangle\langle\Phi_2|). \tag{10}$$

Thereby the radial Hamiltonian of the Rydberg electron in channel j is given by $\mathbf{h}_{jj} = -\tfrac{1}{2}(d^2/dr^2) + l_j(l_j + 1)/2r^2 - 1/r$ (l_j is its angular momentum). The short-range potentials $\mathbf{V}_{ij}(r)$ describe electron correlations which arise from the presence of the residual core electrons. The relevant threshold energies in the rotating wave approximation, which are shifted appropriately by ω, are denoted ε_{cj}. The Rabi frequency Ω characterizes the laser-induced core coupling between channels 1 and 2 and is assumed to be real valued for the sake of simplicity.

The stochastic part of the atomic dynamics is described by the Lindblad operator

$$L = \sqrt{\kappa}|\Phi_1\rangle\langle\Phi_2|, \tag{11}$$

which characterizes the spontaneous decay of the ionic core from state $|\Phi_2\rangle$ to state $|\Phi_1\rangle$ by the spontaneous emission of a photon.

B. Semiclassical path representation of N-photon transition amplitudes

The optical Bloch equation, Eq. (7), may be solved numerically by expanding the density operator into a basis set of operators constructed from the Rydberg system eigenfunctions. This method, however, is only applicable efficiently in cases where the number of energy eigenstates involved in the dynamical process is sufficiently small. Another approach to the solution of Eq. (7) which was originally proposed by Mollow [16] is based on a representation of the density operator in terms of a (fictitious) ensemble of wave functions. Pursuing this approach the appearance of such wave functions allows one to make use of semiclassical methods which have already proven useful for the description of the dynamics of electronic wave functions and threshold phenomena in related contexts. On the one hand, from a practical point of view these methods are particularly useful in situations where the number of emitted photons is small and the excitation takes place very close to threshold. Examples of such situations will be given in Sec. III. On the other hand, these semiclassical methods yield physical insights into aspects of the photon emission process which are not obtainable from the direct numerical solution of Eq. (7).

The starting point for the second approach is a formal integration and iteration of Eq. (7). Thereby, $\rho(t)$ can be decomposed into a sum of N-photon contributions, i.e., $\rho(t) = \Sigma_{N=0}^{\infty}\rho^{(N)}(t)$. In the case of an initially prepared pure state $\rho(t_a = 0) = |\psi_g\rangle\langle\psi_g|$ the N-photon contribution $\rho^{(N)}(t)$ can be represented by the statistical mixture of pure states

$$\rho^{(N)}(t) = \int_0^t dt_N \int_0^{t_N} dt_{N-1} \cdots \int_0^{t_2} dt_1 |\psi(t|t_N, \ldots, t_1)\rangle$$

$$\times \langle \psi(t|t_N, \ldots, t_1)|, \qquad (12)$$

with

$$|\psi(t|t_N, \ldots, t_1)\rangle = e^{-iH_{\text{eff}}(t-t_N)} \Theta(t-t_N) L$$

$$\times e^{-iH_{\text{eff}}(t_N - t_{N-1})} \Theta(t_N - t_{N-1})$$

$$\times L \cdots L e^{-iH_{\text{eff}}t_1} \Theta(t_1) |\psi_g\rangle \qquad (13)$$

and $\Theta(t)$ the unit step function. According to Mollow, $|\psi(t|t_N, \ldots, t_1)\rangle$ may be interpreted as describing the state of the atom at time t after N photons have been emitted at times $0 \leq t_1 \leq t_2 \leq \cdots \leq t_N$. With each emission of a photon the state of the ionic core is reduced to its ground state by application of the Lindblad operator L. The dynamics between the photon emission processes is described by the effective (non-self-adjoint) Hamiltonian

$$H_{\text{eff}} = H - (i/2) L^\dagger L. \qquad (14)$$

Inserting Eq. (12) into Eq. (4) it is apparent that the evaluation of $P_{g\to f}(t_b - t_a)$ can be reduced to the evaluation of pump-probe transition amplitudes

$$A_{g\to f}^{(N)}(t|t_N, \ldots, t_1) = \langle \psi_f | \psi(t|t_N, \ldots, t_1)\rangle, \qquad (15)$$

with

$$P_{g\to f}(t) = \sum_{N=0}^{\infty} \int_0^t dt_N \int_0^{t_N} dt_{N-1} \cdots \int_0^{t_2} dt_1$$

$$\times |A_{g\to f}^{(N)}(t|t_N, \ldots, t_1)|^2. \qquad (16)$$

To calculate the pump-probe probability, one has thus finally to sum over all possible photon emission times and all possible numbers of emitted photons. In our context this method is therefore particularly useful if the structure of the problem or the interaction times are such that the number of emitted photons is small.

The main problem in this approach is the evaluation of the time-dependent N-photon transition amplitudes $A_{g\to f}^{(N)}(t|t_N, \ldots, t_1)$. They are related to time-independent N-photon amplitudes $T_{g\to f}^{(N)}(\varepsilon_{N+1}, \ldots, \varepsilon_1)$ via Laplace transform, i.e.,

$$A_{g\to f}^{(N)}(t|t_N, \ldots, t_1) = \left(\frac{i}{2\pi}\right)^{N+1} \int_{-\infty+i0}^{\infty+i0} d\varepsilon_{N+1} \cdots$$

$$\times \int_{-\infty+i0}^{\infty+i0} d\varepsilon_1 e^{-i\varepsilon_{N+1}(t-t_N) - \cdots - i\varepsilon_1 t_1}$$

$$\times \widetilde{\mathcal{E}}_2^*(\varepsilon_{N+1} - \bar{\varepsilon}) T_{g\to f}^{(N)}(\varepsilon_{N+1}, \ldots, \varepsilon_1)$$

$$\times \widetilde{\mathcal{E}}_1(\varepsilon_1 - \bar{\varepsilon}). \qquad (17)$$

The time-independent amplitudes are given by

$$T_{g\to f}^{(N)}(\varepsilon_{N+1}, \ldots, \varepsilon_1)$$

$$= \langle f | \mathbf{d} \cdot \mathbf{e}_2^* \frac{1}{\varepsilon_{N+1} - H_{\text{eff}}} L \cdots L \frac{1}{\varepsilon_1 - H_{\text{eff}}} \mathbf{d} \cdot \mathbf{e}_1 | g \rangle. \qquad (18)$$

For these amplitudes a semiclassical path representation can be derived with the help of MQDT, which expresses them as a sum of amplitudes which are associated with repeated returns of the excited Rydberg electron to the core region and which include effects due to spontaneous emission of photons by the ionic core between successive returns.

To this end, $T_{g\to f}^{(N)}(\varepsilon_{N+1}, \ldots, \varepsilon_1)$ is expressed as a matrix element involving solutions of inhomogeneous Schrödinger equations, i.e.,

$$T_{g\to f}^{(N)}(\varepsilon_{N+1}, \ldots, \varepsilon_1) = \langle \bar{\lambda}(\varepsilon_{N+1}) | L | \lambda(\varepsilon_N, \ldots, \varepsilon_1)\rangle \qquad (19)$$

for $N \geq 1$ with

$$(\varepsilon_1 - H_{\text{eff}}) |\lambda(\varepsilon_1)\rangle = \mathbf{d} \cdot \mathbf{e}_1 | g \rangle,$$

$$(\varepsilon_n - H_{\text{eff}}) |\lambda(\varepsilon_n, \ldots, \varepsilon_1)\rangle = L |\lambda(\varepsilon_{n-1}, \ldots, \varepsilon_1)\rangle,$$

$$(\varepsilon_{N+1}^* - H_{\text{eff}}^\dagger) |\bar{\lambda}(\varepsilon_{N+1})\rangle = \mathbf{d} \cdot \mathbf{e}_2 | f \rangle. \qquad (20)$$

The second of these equations gives a recursive definition of $|\lambda(\varepsilon_N, \ldots, \varepsilon_1)\rangle$ for $N \geq 2$. The corresponding zero-photon amplitude is given by

$$T_{g\to f}^{(0)}(\varepsilon_1) = \langle f | \mathbf{d} \cdot \mathbf{e}_2^* | \lambda(\varepsilon_1)\rangle. \qquad (21)$$

With the help of methods from multichannel quantum defect theory physical solutions of the inhomogeneous Schrödinger equations (20) can be constructed which are valid for distances $r \geq r_c$ of the Rydberg electron from the nucleus. Thereby, r_c denotes a typical core radius which is of the order of a few Bohr radii. These solutions are determined uniquely by the requirements that they have to remain finite for $r \to 0$ as well as for $r \to \infty$. Having determined the solution of Eqs. (20) the matrix element of Eq. (19) can be evaluated with the help of the overlap formula for radial Coulomb wave functions thereby assuming that the dominant contribution to this matrix element comes from distances $r \geq r_c$. Details of this derivation will be outlined in the Appendix. At this point we only want to mention that in contrast to the first and third of Eqs. (20), which have short-ranged inhomogeneities and can be solved with methods derived previously [1,24], the second one has an inhomogeneous term which is nonzero even for large distances of the Rydberg electron from the ionic core. Despite this complication this equation can be solved as this inhomogeneity is a Coulomb function for $r \geq r_c$.

Thus using Eqs. (19)–(21) as a final result the following semiclassical path representations are obtained which are valid for $\text{Im}\varepsilon_n > 0$, $n = 1, \ldots, N+1$:

$$T_{g\to f}^{(0)}(\varepsilon_1) = T_{g\to f}^{(s)} + 2\pi i \, \tilde{\mathcal{D}}_{fe_2}^{(+)} \sum_{M_1=0}^{\infty} e^{2\pi i \tilde{\nu}_1} (\tilde{\chi} e^{2i\pi \tilde{\nu}_1})^{M_1} \tilde{\mathcal{D}}_{ge_1}^{(-)},$$

$$(22)$$

$$T_{g\to f}^{(1)}(\varepsilon_2,\varepsilon_1)=2\pi i\tilde{\boldsymbol{\mathcal{D}}}_{f\mathbf{e}_2}^{(+)}\sum_{M_2=0}^{\infty}\sum_{M_1=0}^{\infty}(e^{2\pi i\tilde{\boldsymbol{\nu}}_2}\tilde{\boldsymbol{\chi}})^{M_2}$$

$$\times\tilde{\mathbf{S}}_{2,1}(\tilde{\boldsymbol{\chi}}e^{2\pi i\tilde{\boldsymbol{\nu}}_1})^{M_1}\tilde{\boldsymbol{\mathcal{D}}}_{g\mathbf{e}_1}^{(-)}, \qquad (23)$$

and

$$T_{g\to f}^{(N)}(\varepsilon_{N+1},\ldots,\varepsilon_1)$$

$$=2\pi i\tilde{\boldsymbol{\mathcal{D}}}_{f\mathbf{e}_2}^{(+)}\sum_{(k_p,\ldots,k_1)}\sum_{M_{N+1}=0}^{\infty}\sum_{M_{k_p}=0}^{\infty}\cdots$$

$$\times\sum_{M_{k_1}=0}^{\infty}\sum_{M_1=0}^{\infty}(e^{2\pi i\tilde{\boldsymbol{\nu}}_{N+1}}\tilde{\boldsymbol{\chi}})^{M_{N+1}}$$

$$\times\tilde{\mathbf{S}}_{N+1,k_p}\tilde{\boldsymbol{\chi}}(e^{2\pi i\tilde{\boldsymbol{\nu}}_{k_p}}\tilde{\boldsymbol{\chi}})^{M_{k_p}}$$

$$\times\tilde{\mathbf{S}}_{k_p,k_{p-1}}\cdots\tilde{\boldsymbol{\chi}}(e^{2i\pi\tilde{\boldsymbol{\nu}}_{k_1}}\tilde{\boldsymbol{\chi}})^{M_{k_1}}$$

$$\times\tilde{\mathbf{S}}_{k_1,1}(\tilde{\boldsymbol{\chi}}e^{2\pi i\tilde{\boldsymbol{\nu}}_1})^{M_1}\tilde{\boldsymbol{\mathcal{D}}}_{g\mathbf{e}_1}^{(-)} \qquad (24)$$

for $N\geq 2$. These general semiclassical path representations of the time-independent N-photon amplitudes are a main result of this article.

All matrices with a tilde refer to components in the basis of photon-dressed core states $|\tilde{\Phi}_i\rangle$ [2,12]. In the case of a real-valued Rabi frequency these photon-dressed core states are related to the bare core states $|\Phi_j\rangle$ by an orthogonal transformation $\mathbf{O}$ with complex matrix elements, i.e., $|\tilde{\Phi}_i\rangle=\Sigma_{j=1,2,3}\mathbf{O}_{ij}^T|\Phi_j\rangle$. The orthogonal transformation $\mathbf{O}$ diagonalizes the laser-induced coupling of the ionic core, i.e.,

$$\mathbf{O}^T[\boldsymbol{\varepsilon}_c-i\kappa/2|\Phi_2\rangle\langle\Phi_2|-\tfrac{1}{2}\Omega(|\Phi_2\rangle\langle\Phi_1|+|\Phi_1\rangle\langle\Phi_2|)]\mathbf{O}$$

$$=\tilde{\boldsymbol{\varepsilon}}_c. \qquad (25)$$

The diagonal matrix $\tilde{\boldsymbol{\varepsilon}}_c$ contains the complex energies of the dressed states of the ionic core. The (energy-normalized) photoionization and recombination dipole matrix elements into these dressed channels are denoted by the column vectors $\tilde{\boldsymbol{\mathcal{D}}}_{g\mathbf{e}_1}^{(-)}=\mathbf{O}^T\boldsymbol{\mathcal{D}}_{g\mathbf{e}_1}^{(-)}$ and $\tilde{\boldsymbol{\mathcal{D}}}_{f\mathbf{e}_2}^{(+)T}=\mathbf{O}^T\boldsymbol{\mathcal{D}}_{f\mathbf{e}_2}^{(+)T}$. For the excitation scheme of Fig. 1(a) the bare dipole matrix elements are given by $\boldsymbol{\mathcal{D}}_{g\mathbf{e}_1}^{(-)T}=(\mathcal{D}_{g\mathbf{e}_1}^{(-)},0,0)$ and $\boldsymbol{\mathcal{D}}_{f\mathbf{e}_2}^{(+)}=(\mathcal{D}_{f\mathbf{e}_2}^{(+)},0,0)$.

The scattering matrix is determined by $\tilde{\boldsymbol{\chi}}=\mathbf{O}^T\boldsymbol{\chi}\mathbf{O}$ and describes the laser-assisted scattering between the dressed channels which takes place inside the core region. The bare channel scattering matrix is defined as the unitary symmetric matrix

$$\boldsymbol{\chi}=\begin{pmatrix} e^{2\pi i\mu_1} & 0 & 0 \\ 0 & e^{2\pi i\mu_2} & \chi_{23} \\ 0 & \chi_{32} & \chi_{33} \end{pmatrix}. \qquad (26)$$

In the case considered here, the matrix elements χ_{1j} and χ_{j1}, $j=2,3$ are equal to zero, as channel 1 and channels 2,3 are of opposite parity, respectively, and cannot be coupled by electron correlation effects. The matrix elements χ_{23} and χ_{32} characterize the extent of configuration interaction between channels 2 and 3 leading to autoionization of channel 2. Due to unitarity, the quantum defect μ_2 has a

positive imaginary part, in general, which is related to the autoionization rate of the mean excited Rydberg state by $\Gamma_{\bar{\nu}}=4\pi\,\mathrm{Im}(\mu_2)/T_{\mathrm{orb}}$ [17]. The mean wave packet orbit time is denoted by $T_{\mathrm{orb}}=2\pi\bar{\nu}^3$ with the mean excited quantum number $\bar{\nu}=[2(\varepsilon_1-\bar{\varepsilon})]^{-1/2}$ and the threshold of the bare channel 1 ε_1. As the pump-probe and continuous-wave–laser interactions merely affect channels 1 and 2, only the parameters μ_1 and μ_2 of the scattering matrix enter explicitly into calculations of the pump-probe signal.

The smooth part of the zero-photon amplitude is denoted by $T_{g\to f}^{(s)}$ and is essentially given by $i\pi\tilde{\boldsymbol{\mathcal{D}}}_{f\mathbf{e}_2}^{(+)}\tilde{\boldsymbol{\chi}}^{-1}\tilde{\boldsymbol{\mathcal{D}}}_{g\mathbf{e}_1}^{(-)}$. The diagonal 3×3 matrix $e^{2\pi i\tilde{\boldsymbol{\nu}}_k}$ has elements

$$(e^{2\pi i\tilde{\boldsymbol{\nu}}_k})_{jj}=\exp\{2\pi i[2(\tilde{\varepsilon}_{cj}-\varepsilon_k)]^{-1/2}\}.$$

The matrices $\tilde{\mathbf{S}}_{m,k}$ are defined in Eq. (A17) of the Appendix. Their physical significance and the definition of the first sum of Eq. (24) are explained below.

In the spirit of recently developed semiclassical path representations the expressions (22)–(24) for the N-photon transition amplitudes may be interpreted as describing the time evolution of the Rydberg wave packet in terms of repeated returns to the nucleus. Thereby, all the various possibilities are taken into account by which N photons can be emitted spontaneously by the ionic core with respect to the course of the wave packet returns as explained below.

The physical contents of Eq. (22) are already well known from previous work [2]: after the initial excitation those fractions of the wave packet which are excited into closed channels perform repeated orbital round-trips around the nucleus. On each complete round-trip such a fraction acquires a phase of magnitude $2\pi(\nu_1)_{jj}$. Thereby, the quantity $2\pi(\nu_1)_{jj}$ is equal to the classical action of motion along a purely radial Kepler orbit with zero angular momentum and energy $\varepsilon-\tilde{\varepsilon}_{cj}<0$. At each return to the core, the wave packet can be scattered into other channels due to electron correlation effects. This is described by the matrix $\tilde{\boldsymbol{\chi}}$. Alternatively, it may be deexcited to the final state $|f\rangle$. An emission of spontaneous photons does not occur.

The case in which one photon is emitted during the time evolution of the wave packet is described by Eq. (23). This transition amplitude is represented as a sum over all different ways in which the initially prepared wave packet first performs $M_1\geq 0$ complete round-trips, then experiences the spontaneous photon emission by the ionic core during the next round-trip and subsequently performs again $M_2\geq 0$ complete round-trips before it is deexcited to the final state $|f\rangle$. The effect of the photon emission process by the ionic core is described by the matrix $\tilde{\mathbf{S}}_{2,1}$. To a very good degree of approximation it is given by

$$\tilde{\mathbf{S}}_{2,1}\simeq\int_0^T d\tau' e^{2\pi i\tilde{\boldsymbol{\nu}}_2(1-\tau'/T)}(e^{-i\pi/2}\tilde{\mathbf{L}})e^{2\pi i\tilde{\boldsymbol{\nu}}_1\tau'/T}, \qquad (27)$$

where T has to be taken equal to $(t_b-t_a)/(M_2+M_1+1)$ when performing the Laplace transform of Eq. (17). In this physically transparent description it is taken into account that the photon emission may take place at any time $0\leq\tau'\leq T$ between two successive returns of the wave packet

to the core. At this time the electron has acquired a phase of magnitude $[2\pi\widetilde{\nu}_1\tau'/T]$. The effect of the spontaneous emission is then described through the action of the Lindblad operator $\widetilde{\mathbf{L}}=\mathbf{O}^T\mathbf{L}\,\mathbf{O}$, where $\mathbf{L}_{12}=\sqrt{\kappa}$, $\mathbf{L}_{ij}=\mathbf{O}$ otherwise. In addition, the emission is accompanied by a phase change of magnitude $(-\pi/2)$. After the emission the wave packet accumulates a further phase of magnitude $(2\pi\widetilde{\nu}_2(1-\tau'/T))$ during its subsequent way to the core. As the photon emission process can take place at any time between two successive returns to the core the amplitudes associated with all possible values of the effective jump time τ' have to be added coherently as described by Eq. (27).

Equation (24) for the N-photon amplitude may be interpreted analogously. The first sum has to be carried out over all p-tuples $(k_p,\ldots,k_1)$ with $N\geq k_p>\cdots>k_1\geq2$ and $N-1\geq p\geq1$ which can be formed from all possible subsets of $\{N,\ldots,2\}$ and over the empty set which corresponds to the terms containing $\widetilde{\mathbf{S}}_{N+1,1}$ only. Every single summand then describes a process in which the wave packet first performs M_1 complete round-trips, during the next round-trip experiences $(k_1-1)\geq1$ spontaneous photon emissions (characterized by $\widetilde{\mathbf{S}}_{k_1,1}$), then again performs M_2 complete round-trips followed by the emission of $(k_2-k_1)\geq1$ photons during the next one, and so on. Before the deexcitation the wave packet finally performs M_{N+1} complete round-trips following the emission of $(N+1-k_p)\geq1$ photons during the preceding round-trip. This physical interpretation of the quantities $\widetilde{\mathbf{S}}_{m,k}$ follows from their approximate representation as

$$
\begin{aligned}
\widetilde{\mathbf{S}}_{m,k}\simeq &\int_0^T d\tau_k\int_{\tau_k}^T d\tau_{k+1}\cdots\int_{\tau_{m-2}}^T d\tau_{m-1}e^{2\pi i\widetilde{\nu}_m(T-\tau_{m-1})/T}\\
&\times(e^{-i\pi/2}\widetilde{\mathbf{L}})e^{2\pi i\widetilde{\nu}_{m-1}(\tau_{m-1}-\tau_{m-2})/T}\\
&\times(e^{-i\pi/2}\widetilde{\mathbf{L}})\cdots(e^{-i\pi/2}\widetilde{\mathbf{L}})e^{2\pi i\widetilde{\nu}_{k+1}(\tau_{k+1}-\tau_k)/T}\\
&\times(e^{-i\pi/2}\widetilde{\mathbf{L}})e^{2\pi i\widetilde{\nu}_k\tau_k/T},
\end{aligned}\tag{28}
$$

which is an immediate generalization of Eq. (27) to the case of the emission of $(m-k)\geq1$ spontaneous photons during one round-trip. By the first sum of Eq. (24) all different ways of emitting N photons during the evolution of the wave packet with respect to its returns to the nucleus are combined coherently. In analogy to Eq. (27), T has to be taken equal to t_b-t_a divided by the total number of wave packet revolutions between excitation and detection.

Inserting Eqs. (22–24) into Eq. (17) the time dependent N-photon pump-probe transition amplitudes are obtained from which the pump-probe signal can be evaluated by Eq. (16). This method of solution is particularly useful in cases in which only a few photon emission processes are relevant.

The actual numerical calculation of N-photon contributions with the help of these semiclassical path representations is especially convenient if the excitation takes place in the immediate vicinity of the threshold so that a very large or even infinite number of energy eigenstates is involved in the wave packet dynamics. It has to be noted, however, that for accurate calculations also the contributions of the integration in the lower complex half planes (where the integration paths have to be chosen from ∞ to $-\infty$ below all branch cuts) have to be taken into account [25]. These contributions have been omitted in the above discussion for the sake of clarity. Another way of calculating the N-photon contributions starts from the alternative representation (A14) of the N-photon amplitudes which is derived in the Appendix. The time-dependent amplitudes are obtained from this representation in the usual way in terms of residue and branch cut contributions [24]. In cases in which the wave packet is confined energetically to a region well below the thresholds all terms containing branch cut contributions can be neglected and the time-dependent amplitudes are calculated as a sum over residues which is determined by the $(p=N-1)$-tuple contribution to the sum in Eq. (A14).

III. TIME EVOLUTION OF RYDBERG WAVE PACKETS UNDER THE INFLUENCE OF SPONTANEOUS EMISSION PROCESSES

In this section the influence of spontaneous photon emission processes by the ionic core on the time evolution of Rydberg wave packets is studied with the help of the theoretical methods developed in Sec. II. In order to demonstrate characteristic physical effects first of all a simple case is considered in Sec. III A in which the laser-induced core coupling is turned off and two channels are coupled only by the spontaneous decay of the core. In Sec. III B the influence of resonance fluorescence of the ionic core on the dynamics of an electronic Rydberg wave packet is discussed. Results on the influence of spontaneous photon emission on laser-induced suppression of autoionization and the long-time-behavior of an electronic Rydberg wave packet are presented.

A. Wave packet dynamics and spontaneously decaying core

In this subsection we consider the simplified excitation scheme of Fig. 1(b). There, the laser-induced core coupling is turned off and autoionization is neglected. The wave packet is prepared in channel 2 from which it can only make a transition to channel 1, where it is detected, through the spontaneous decay of the ionic core. This pump-probe detection scheme is particularly sensitive to the details of the photon-emission process of the ionic core and its influence on the dynamics of the initially prepared electronic Rydberg wave packet. The pump-probe probability is given exclusively by the one-photon contribution in Eq. (16). From the discussion in Sec. II together with Eq. (A17), it follows that in this case the relevant time-dependent transition amplitude can be written as

$$
\begin{aligned}
A_{g\to f}^{(1)}(t|t_1)=&-\frac{1}{2\pi i}\sum_{M_2,M_1=0}^\infty e^{2\pi i(M_2\mu_2+M_1\mu_1)}\\
&\times\int_{-\infty+i0}^{\infty+i0}d\varepsilon_2\int_{-\infty+i0}^{\infty+i0}d\varepsilon_1\mathcal{E}_2^*(\varepsilon_2-\overline{\varepsilon})\\
&\times\mathcal{D}_{f\mathbf{e}_2}^{(+)}e^{2\pi iM_2\nu_2}\frac{e^{2\pi i\nu_2}-e^{2\pi i\nu_1}}{\varepsilon_2-\varepsilon_{T2}+i\kappa/2-\varepsilon_1+\varepsilon_{T1}}\\
&\times e^{2\pi iM_1\nu_1}\mathcal{D}_{g\mathbf{e}_1}^{(-)}\mathcal{E}_1(\varepsilon_1-\overline{\varepsilon})e^{-i\varepsilon_2(t-t_1)-i\varepsilon_1 t_1},
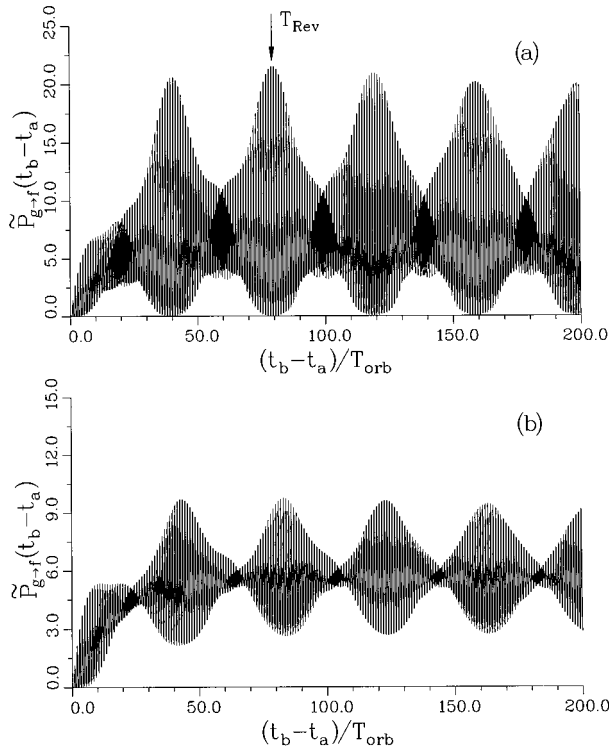\end{aligned}
$$

$$\tag{29}$$

FIG. 2. Scaled pump-probe probability $\widetilde{P}_{g\to f}=P_{g\to f}/|\mathcal{D}_{fe_2}^{(+)}\mathcal{E}_2^{(0)}\mathcal{D}_{ge_1}^{(-)}\mathcal{E}_1^{(0)}\tau|^2$ as a function of the time delay (t_b-t_a) for the excitation scheme of Fig. 1(b) and $\mu_1=\mu_2=0.0$ (a); $\mu_1=0.0$, $\mu_2=0.5$ (b). The other parameters are $\kappa T_{\text{orb}}=1/15$, $\bar{\nu}_2=119$ ($T_{\text{orb}}=256$ ps), $\tau=0.3T_{\text{orb}}$. The revival time $T_{\text{rev}}=\frac{2}{3}\bar{\nu}_2 T_{\text{orb}}$ is also indicated in (a).

where the notation with normal characters without tilde refers to the corresponding individual bare channel quantities. The bare channel thresholds are denoted ε_{T1} and ε_{T2}. The semiclassical path representation is now particularly helpful to explain some characteristic features of the combined influence of the spontaneous decay of the initially excited core and the shakeup process on the electronic Rydberg wave packet.

The effect of this influence is illustrated in Fig. 2 where the pump-probe probability for the excitation scheme described above is shown for two examples which are distinct only in the difference between the quantum defects of the two channels involved. In Fig. 2(a) the two quantum defects are equal. It can be shown that the one-photon transition amplitude $A_{g\to f}^{(1)}(t|t_1)$ is then given by the product of the zero-photon amplitude at time t describing the detection of the wave packet if it was prepared in channel 1 and an envelope factor $e^{-\kappa t_1/2}$ characterizing the decay of the excited core. This implies that for times $\kappa t \gg 1$, i.e., after the spontaneous decay of the core, the wave packet has simply passed from channel 2 to channel 1 without any further modification. In particular, its initial coherence is completely maintained.

In the presence of shakeup processes the coherence of the wave packet after the core decay is diminished. This is shown in Fig. 2(b) where the difference in quantum defects is maximal, i.e., $\mu_2-\mu_1=0.5$. The diminution of coherence can be inferred from the decrease of the amplitudes of the
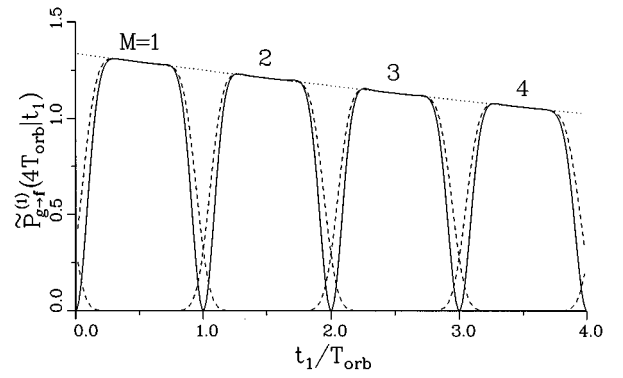
FIG. 3. Scaled conditional one-photon pump-probe probability $\widetilde{P}_{g\to f}^{(1)}(t_b-t_a|t_1)=P_{g\to f}^{(1)}(t_b-t_a|t_1)/(|\mathcal{D}_{fe_2}^{(+)}\mathcal{E}_2^{(0)}\mathcal{D}_{ge_1}^{(-)}\mathcal{E}_1^{(0)}\tau|^2/T_{\text{orb}})$ as a function of t_1 for the parameters of Fig. 2 and $t_b-t_a=4T_{\text{orb}}$. Dotted curve: $\mu_1=\mu_2=0.0$; full curve: $\mu_1=0.0$, $\mu_2=0.5$. The dashed curves show the contributions to $P_{g\to f}^{(1)}(t_b-t_a|t_1)$ from spontaneous emission during the Mth round-trip of the wave packet ($M=1,2,3,4$) as evaluated from Eq. (29).

recurrence contributions in the pump-probe signal. It may be explained with the help of the semiclassical path representation by the following picture: according to Eq. (16) the pump-probe probability, and in analogy the wave packet, at time t may be partitioned into contributions from all spontaneous emission times t_1 with $0\le t_1\le t$. Each of these contributions is represented by Eq. (29) as a sum of terms describing wave packet fractions after a total number of M_1+1+M_2 complete orbital round-trips and spontaneous photon emission during the (M_1+1)th round-trip. The shakeup effects are incorporated into these terms only through a global phase of magnitude $2\pi(M_2\mu_2+M_1\mu_1)$ which arises because of the core scatterings. At given times $(t;t_1)$ several different (M_1,M_2) terms will contribute to the sum of Eq. (29), in general. Only in the case of equal quantum defects are the phase relationships between all wave packet fractions such that their superposition describes a coherent wave packet through Eqs. (16) and (29). In the presence of shakeup the phase relationships are disturbed so that the decoherence of the wave packet can be attributed to interference effects between wave packet fractions having experienced different numbers of core scatterings in the excited and the unexcited channel. As a consequence the decoherence is the more pronounced the larger the number of core scatterings in the excited channel before the spontaneous emission, i.e., the smaller κ.

To illustrate these considerations, in Fig. 3 the conditional one-photon pump-probe probability $P_{g\to f}^{(1)}(t|t_1)=|A_{g\to f}^{(1)}(t|t_1)|^2$ is shown for the examples of Fig. 2 at time $t=4T_{\text{orb}}$ as a function of t_1. In this case only terms with $M_1+1+M_2=4$ contribute significantly to the sum of Eq. (29). At times t_1 around nT_{orb} the terms with $M_1=n-1$ and $M_1=n$ interfere constructively in the case of equal quantum defects and destructively for $\mu_2-\mu_1=0.5$.

B. Wave packet dynamics and resonance fluorescence of the ionic core

1. Spontaneous emission and autoionization

In this subsection we discuss a slightly different experimental setup which is particularly sensitive to effects of

spontaneous photon emission and which could be realized on the basis of present-day technology. It is shown that the effects can be analyzed efficiently with the help of the theoretical methods developed in Sec. II.

In the excitation scheme of Fig. 1(a) the lifetime of a Rydberg wave packet evolving in channels 1 and 2 is of the order of the inverse autoionization rate $\Gamma_{\bar{\nu}}^{-1}$, in general. However, as it was shown recently [3], it is possible to increase this lifetime by orders of magnitude if one synchronizes core and wave packet dynamics by choosing the orbit time T_{orb} equal to an integer multiple of the Rabi period T_{Rabi}. If initially the wave packet is prepared with the core in its ground state, in the course of its successive returns to the nucleus the Rydberg electron will always encounter an unexcited core so that the wave packet is virtually stable and autoionization occurs only with a very small rate $\Gamma_s \ll \Gamma_{\bar{\nu}}$. If now spontaneous photon emission by the excited core is possible, in the simplest case, i.e., $T_{orb} = T_{Rabi}$, the first spontaneous photon will predominantly be emitted (thus reducing the core to the ground state) when the wave packet is at its outer turning point because the core is then in its excited state. This means that at its subsequent returns to the nucleus the wave packet will face an excited core so that it will decay rapidly on a time scale of the order of $\Gamma_{\bar{\nu}}^{-1}$. In the case of $\Gamma_s \ll \kappa$ the overall decay of the Rydberg population which is reflected in the decay of the pump-probe signal therefore occurs on a time scale given by κ^{-1}. As typically $\kappa \ll \Gamma_{\bar{\nu}}$, it is rather improbable that a second photon is emitted spontaneously before autoionization takes place. The relevant physical processes are therefore very well described by taking into account the zero- and one-photon contributions only.

The manifestation of spontaneous photon emission effects through enhancement of the decay of the Rydberg population would still be difficult to observe under realistic conditions in conventional pump-probe experiment due to the smallness of typical spontaneous emission rates κ. Therefore in the following we turn to the discussion of the time-dependent autoionization rate $\gamma(t)$ of the Rydberg atom. This quantity is much more sensitive to the effects of spontaneous photon emission. Furthermore, a streak-camera technique for the measurement of ionization rates such as $\gamma(t)$ was developed recently by Lankhuijzen and Noordam [26].

In the three-channel model of Fig. 1(a) the time-dependent autoionization rate is given by the change of the population of channel 3, i.e.,

$$\gamma(t) = \frac{d}{dt}\mathcal{P}_3(t) = -\frac{d}{dt}[\mathcal{P}_1(t) + \mathcal{P}_2(t)], \quad (30)$$

with $\mathcal{P}_i(t)$ the total population of channel i at time t. A straightforward way to determine this rate would consist in calculating the populations $\mathcal{P}_1(t)$ and $\mathcal{P}_2(t)$ by solving the master equation (7) by means of a finite basis set expansion. For this purpose the influence of the (flat) autoionization continuum on the bound channels 1 and 2 can be described by an optical potential [15,27]. It should be mentioned that this approach is only valid as long as the initial wave packet is exclusively prepared in the bound channels and the Lindblad operator (11) acts within channels 1 and 2 only.

However, the autoionization rate $\gamma(t)$ may also be determined in a way which is often computationally more effi-

cient and which also yields a clear physical picture of the physical processes involved by making use of the methods derived in Sec. II. In the framework of Mollow's approach the total rate $\gamma(t)$ may be decomposed into a sum of N-photon contributions $\gamma^{(N)}(t)$ which in turn can be represented as integrals over conditional autoionization rates $\gamma^{(N)}(t|t_N, \ldots, t_1)$, i.e.,

$$\gamma^{(N)}(t) = \int_0^t dt_N \cdots \int_0^{t_2} dt_1 \gamma^{(N)}(t|t_N, \ldots, t_1). \quad (31)$$

Approximating the continuum channel population by the part outside the core region the conditional autoionization rate is given by

$$\gamma^{(N)}(t|t_N, \ldots, t_1)$$
$$= \frac{1}{2i} W[\psi_3^{(N)*}(r,t|t_N, \ldots, t_1), \ \psi_3^{(N)}(r,t|t_N, \ldots, t_1)]_{r_c},$$
$$(32)$$

with $W[\phi, \psi]$ the Wronskian of ϕ and ψ and $\psi_3^{(N)}$ the conditional continuum electron wave function. Thus with the help of MQDT and the results of the Appendix one obtains from the above expression for the case that in channels 1 and 2 only bound states are populated significantly the result

$$\gamma^{(N)}(t|t_N, \ldots, t_1) = \left(\frac{1}{2\pi}\right)^{2N+1}(1 - e^{-4\pi \operatorname{Im}\mu_2})$$

$$\times \left| \int_{-\infty+i0}^{\infty+i0} d\varepsilon_{N+1} \cdots d\varepsilon_1 \right.$$

$$\times e^{-i\varepsilon_{N+1}(t-t_N) - \cdots - i\varepsilon_1 t_1}(0,1,0)\mathbf{O}$$

$$\times (e^{-2\pi i \tilde{\nu}_{N+1}} - \tilde{\chi})^{-1} \widetilde{\mathbf{W}}_{N+1,N}$$

$$\times (e^{-2\pi i \tilde{\nu}_N} - \tilde{\chi})^{-1} \cdots \widetilde{\mathbf{W}}_{2,1}$$

$$\times \left. (e^{-2\pi i \tilde{\nu}_1} - \tilde{\chi})^{-1} \tilde{\mathbf{D}}_{g\mathbf{e}_1}^{(-)} \tilde{\boldsymbol{\mathcal{E}}}_1(\varepsilon_1 - \bar{\varepsilon}) \right|^2.$$

$$(33)$$

The matrices $\widetilde{\mathbf{W}}_{m,n}$ are defined in Eq. (A15). The integrations over $\varepsilon_{N+1}, \ldots, \varepsilon_1$ may be performed with the theorem of residues. It should be mentioned that Eq. (33) is of a form very similar to the corresponding expression for the pump-probe probability from which it only differs by the replacement of $\tilde{\mathcal{E}}_2^* \mathbf{D}_{f\mathbf{e}_2}^{(+)}$ by the vector $(0,1,0)\mathbf{O}$ times a constant because only channel 2 is autoionizing. Similar expressions may also be obtained for the populations of channels 1 and 2.

In Fig. 4(a) (full curve) $\gamma(t)$ is shown for an example with parameters $\bar{\nu}_1 = 73$, $\mu_1 = 0.0$, $\mu_2 = 0.50 + i0.10$, and a spontaneous lifetime of $\kappa^{-1} = 7$ ns $= 118 T_{orb}$ which is a typical value for alkaline earth atoms. Comparison with the autoionization rate for $\kappa = 0$ in Fig. 4(a) (dotted curve) shows the significant influence of spontaneous emission on the behavior of $\gamma(t)$ which is manifest already for times of the order of T_{orb}. This means that these effects might be observed not only when the core transition is driven by a cw-laser pulse but also in the case of a core excitation with a ns pulse as discussed in Ref. [3]. Further calculations show
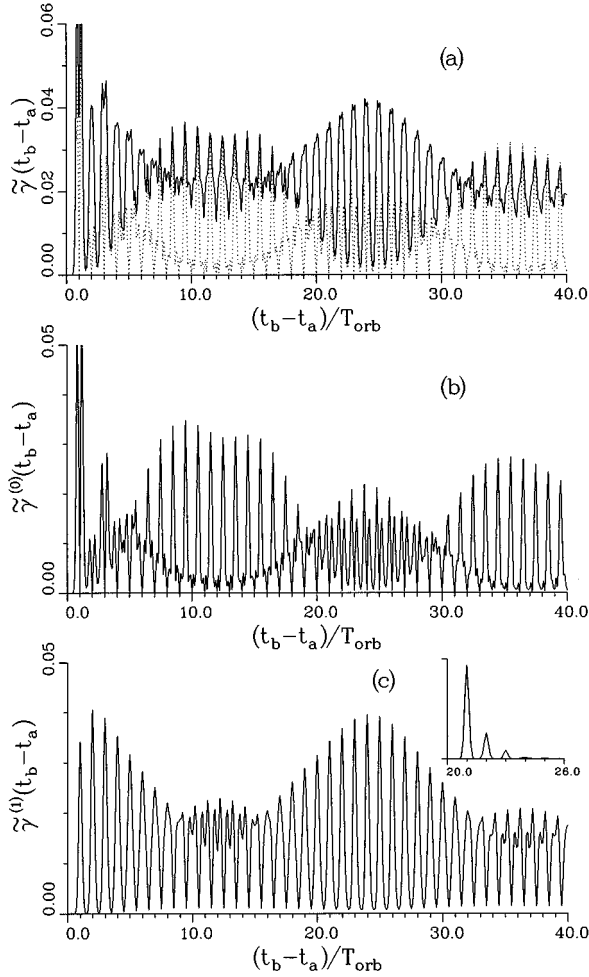
FIG. 4. Autoionization under the condition of period matching of orbit time and Rabi period in the presence of spontaneous emission for parameters $T_{\text{Rabi}} = T_{\text{orb}}$, $\kappa T_{\text{orb}} = 1/118$, $\bar{\nu}_1 = 73$ ($T_{\text{orb}} = 59$ ps), $\mu_1 = 0.0$, $\mu_2 = 0.50 + i0.10$, $\tau = 0.4T_{\text{orb}}$, $\Delta = \varepsilon_{T2} - \varepsilon_{T1} - \omega = 0$ with the bare channel thresholds $\varepsilon_{T1}, \varepsilon_{T2}$. (a) Total scaled autoionization rate $\tilde{\gamma} = \gamma T_{\text{orb}} \tau / |\mathcal{D}_{g\mathbf{e}_1}^{(-)} \mathcal{E}_1^{(0)}|^2$ as obtained from the optical Bloch equations (full curve), total rate for $\kappa = 0$ (dotted). (b) and (c) Zero- and one-photon contributions $\tilde{\gamma}^{(0)}$ and $\tilde{\gamma}^{(1)}$. Inset in (c): conditional autoionization rate $\gamma^{(1)}(t|t_1 = 20.5T_{\text{orb}})$.

that, as expected, the total autoionization rate is accurately described by the sum of the zero- and one-photon contributions up to times of the order of several κ^{-1}. The reason for the sensitivity of the autoionization rate to spontaneous emission effects is the fact that before the photon emission the probability of autoionization is rather low because of the described stabilization effect while after the emission the atom autoionizes very rapidly so that $\gamma^{(1)}(t)$ may become comparable to $\gamma^{(0)}(t)$ even if the spontaneous emission rate is small. The notion of rapid autoionization after spontaneous emission is confirmed by the inset in Fig. 4(c) which shows the conditional autoionization rate $\gamma^{(1)}(t|t_1)$ as a function of $t > t_1$ for fixed t_1. It should also be noted that the autoionization rate of an excited wave packet scales with the inverse of its mean orbit time while the spontaneous emission rate is independent of it. This means that the importance of spontaneous emission effects, i.e., the contribution of $\gamma^{(1)}(t)$ rela-

tive to $\gamma^{(0)}(t)$, can easily be varied by altering the mean excited quantum number.

A further confirmation for the above discussion of the ionization dynamics is obtained from the time evolution of the zero- and one-photon autoionization rates $\gamma^{(0)}(t)$ and $\gamma^{(1)}(t)$ which are depicted in Figs. 4(b) and 4(c). The zero-photon rate is always very small exactly at times nT_{orb} as the core is then deexcited. However, for the first few round-trips $\gamma^{(0)}(t)$ is peaked in the vicinity of times nT_{orb} whereas later on peaks appear at times $(n + \frac{1}{2})T_{\text{orb}}$. The pattern is repeated after approximately 25 periods due to quantum mechanical revival effects. A detailed discussion of the wave packet dynamics is given in [28]. The behavior of the one-photon rate is less complicated. The autoionization displays distinct maxima and minima at times nT_{orb} and $(n + \frac{1}{2})T_{\text{orb}}$, respectively, according to whether the core is excited or unexcited.

2. Long-time behavior of atomic dynamics

The emission of more than one spontaneous photon is rather unlikely in a typical pump-probe experiment due to the inevitable autoionization processes. Nevertheless, from a more theoretical point of view it might well be worthwhile to study on a longer time scale the effect of spontaneous emission on the Rydberg wave packet dynamics in situations where autoionization is neglected in order to get a more thorough understanding of the influence of this dissipative process on the time evolution of the atomic system. As is already apparent from the discussion in Sec. III A, the interplay between spontaneous emission and shakeup processes is crucial in this context. Modifications of the short-time behavior due to spontaneous emission are discussed in Ref. [25].

In the absence of shakeup processes, i.e., for $\mu_1 = \mu_2$, the optical Bloch equations can easily be decoupled into a set of two-state-like Bloch equations each describing the time evolution of the 4×4 subdensity matrix belonging to a pair of Rydberg states. When the system has settled to the steady state, i.e., $\kappa(t_b - t_a) \gg 1$, the pump-probe signal for resonant core excitation ($\varepsilon_{T1} + \omega = \varepsilon_{T2}$) is given by the expression

$$
\begin{aligned}
P_{g \to f}(t_b - t_a) = & \frac{1}{2}(M_{++}M_{++}^* + M_{--}M_{--}^* + M_{-+}M_{-+}^* \\
& + M_{+-}M_{+-}^*) \\
& + \frac{-x^2 - 2ix}{4 + 2x^2}(M_{+-}M_{++}^* + M_{--}M_{-+}^*) \\
& + \frac{-x^2 + 2ix}{4 + 2x^2}(M_{++}M_{+-}^* + M_{-+}M_{--}^*),
\end{aligned}
$$

(34)

with $x = \kappa/\Omega$ and

$$
\begin{aligned}
M_{\beta\beta'} = & \sum_l \langle f | \mathbf{d} \cdot \mathbf{e}_f^* | l\beta \rangle \tilde{\mathcal{E}}_b^*(\varepsilon_l^{\beta} - \bar{\varepsilon}) e^{-i\varepsilon_l(t_b - t_a)} \tilde{\mathcal{E}}_a(\varepsilon_l^{\beta'} - \bar{\varepsilon}) \\
& \times \langle l\beta' | \mathbf{d} \cdot \mathbf{e}_g | g \rangle.
\end{aligned}
$$

Thereby, β denotes one of the dressed channels ($+$ or $-$), and the summation extends over all Rydberg states $|l\beta\rangle$ and

$|l\beta'\rangle$ in the dressed channels β and β', respectively. The energies are given by $\varepsilon_l = -1/[2(l-\mu)^2]$ and $\varepsilon_l^\pm = \varepsilon_l \pm \Omega/2$.

Expression (34) for the long-time behavior of the pump-probe signal may be interpreted as follows: the dressed states of the system consisting of the atom and the cw-laser field are given by $|k\pm\rangle = 1/\sqrt{2}(|k1\rangle \pm |k2\rangle)$ with $|k1(2)\rangle$ denoting the eigenstates of the bare atomic channels with principal quantum number k. The initial (coherent) Rydberg wave function created by the first short laser pulse is a superposition of states $\{|k+\rangle\}$ and $\{|l-\rangle\}$ where the sets K and L of relevant principal quantum numbers k and l may be different from each other due to the Rabi splitting of the core states. The spontaneous emission processes now lead to a population transfer from states $\{|k+\rangle\}$ to states $\{|k-\rangle\}$ and from $\{|l-\rangle\}$ to $\{|l+\rangle\}$, respectively, as there are no shakeup processes. The result of this population transfer is described by the amplitudes $M_{\beta\beta'}$. Equation (35) for the amplitudes shows that the internal coherence of the wave packet fractions which change or remain in their dressed channels is completely maintained. This is due to the fact that the spontaneous emission does not destroy the basic phase relationship between Rydberg states of different principal quantum numbers m,n which is given by the factor $\exp[-i(\varepsilon_m - \varepsilon_n)t]$.

As an example of the consequences of this time evolution, consider a case in which $\Omega \gg \kappa, 1/\tau$ (with τ the temporal width of the laser envelope). Under these conditions the terms in the third and fourth lines of Eq. (34) which express interference effects between the wave packet fractions created in different dressed channels and detected in either the $+$ or $-$ channel can be neglected. If pump and probe signal are centered at the same mean energy $\bar{\varepsilon}$ one obtains a signal $P_{g\to f}(t) = \frac{1}{2}(M_{++}M_{++}^* + M_{--}M_{--}^*)$, i.e., an incoherent sum of wave packet contributions prepared and detected in channels $+$ and $-$. However, if pump and probe pulses are centered at energies $\bar{\varepsilon}$ and $\bar{\varepsilon}+\Omega$ ($\bar{\varepsilon}-\Omega$) the signal is given by $\frac{1}{2}M_{+-}M_{+-}^*$ ($\frac{1}{2}M_{-+}M_{-+}^*$), i.e., one observes the wave packets which are created through the spontaneous emission processes. These wave packets have the same orbit time as the faster (slower) of the wave packets initially created.

In situations where the Rydberg electron evolves under the simultaneous influence of spontaneous emission and shakeup processes simple analytic expressions for the pump-probe signal are not available. Numerical studies indicate that the presence of shakeup processes leads to profound changes in the long-time behavior of the atomic dynamics in comparison with the situation in which such processes are absent. As discussed above in the latter case the atomic population is distributed even under steady-state conditions only over a finite number of states and the initial coherence of the Rydberg states is preserved to a high degree. In contrast to this behavior the influence of shakeup processes leads to a spreading of the atomic population over a continually growing number of Rydberg states while the initial coherence is destroyed. To exemplify these observations Fig. 5 shows the pump-probe signal for the parameters $\mu_2 - \mu_1 = 0.5$, $T_{\mathrm{Rabi}} = 3T_{\mathrm{orb}}$, $\kappa T_{\mathrm{orb}} = 1/5$, and $\bar{\nu}_1 = 171$. The loss of coherence in the atomic system is reflected in the diminution of the wave packet recurrence structures in the
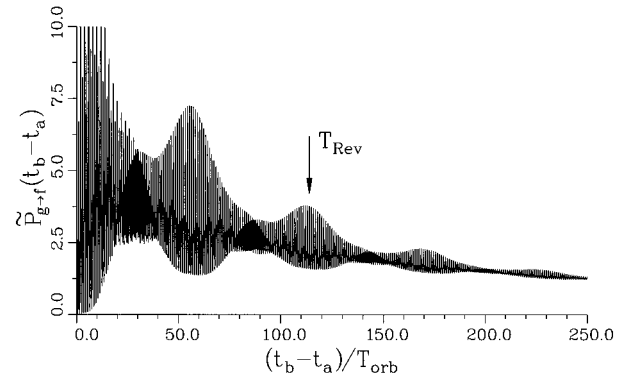

FIG. 5. Scaled pump-probe probability $\widetilde{P}_{g\to f}$ for $\mu_1 = 0.0$, $\mu_2 = 0.5$, $T_{\mathrm{Rabi}} = 3T_{\mathrm{orb}}$, $\kappa T_{\mathrm{orb}} = 1/5$, $\bar{\nu}_1 = 171$ ($T_{\mathrm{orb}} = 760$ ps), $\Delta = 0$, and $\tau = 0.3T_{\mathrm{orb}}$.

pump-probe signal, the gradual decline of the mean signal (averaged over several orbit times) is due to the spreading of the population. The physical process which is responsible for this spreading appears to consist in the fact that in the course of successive spontaneous emission events the atom can go over from one dressed eigenstate to any other one due to the shakeup couplings. This notion is corroborated by the observation that the spread is accelerated if Ω or κ is increased, both of which lead to an enhanced spontaneous emission. However, a similar reasoning could also be applied in situations where spontaneous emission is absent. It could be argued that the stimulated absorption and emission processes should also lead to a spread of the wave function. The fact that such a spread does not occur suggests that the atomic system in this case is in a kind of dynamical balance which prevents it from spreading and which is destroyed by spontaneous emission.

IV. SUMMARY AND CONCLUSION

Motivated by the recent interest in ICE processes in intense laser fields [2,3,12–15] the decohering influence of the spontaneous emission of photons by the ionic core on ICE wave packet dynamics has been investigated.

For this purpose a theoretical approach has been developed which is based on Mollow's pure state analysis of resonance fluorescence and on MQDT. In this way it is possible to obtain semiclassical path representations for atomic transition amplitudes which clearly exhibit the interplay between classical and quantum mechanical aspects of wave packet dynamics in the presence of dissipation. The presented theoretical approach which relies on a decomposition of the relevant transition amplitudes into N-photon contributions is particularly useful in situations in which the number of spontaneously emitted photons is small. For such cases it allows us to circumvent mathematical and numerical problems which arise from the solution of the relevant master equation in Rydberg systems close to a photoionization threshold. Furthermore, each N-photon contribution has physical significance as it can be observed in a coincidence experiment in which not only the time evolution of the Rydberg wave packet but also the number of spontaneously emitted photons is measured.

The presented physical examples demonstrate the intricate

interplay between the (coherent) laser-modified electron correlation effects, such as shakeup and autoionization, which take place inside the core region of the Rydberg system, and the classical aspects of the dynamics of the excited Rydberg electron outside the core region which is interrupted by the (stochastic) spontaneous decay process of the ionic core. In particular, these examples show that the decoherent influence of the stochastic photon emission process on the dynamics of an electronic Rydberg wave packet is the more pronounced the more important shakeup processes are. In the framework of the semiclassical path approach this observation could be explained to arise from modifications of interference effects due to core scattering. Furthermore, it was shown that effects of spontaneous emission can play a significant role in ionization experiments in connection with a recently discussed (coherent) mechanism of laser-induced suppression of autoionization [3]. The analysis of these experiments is performed efficiently in terms of zero- and one-photon contributions which can be obtained directly from our general theoretical results. Thus in view of recent experimental developments [26] besides conventional pump-probe experiments time-dependent studies of ionization rates might also become a valuable experimental tool for studying ICE wave packet dynamics and its modification by stochastic influences.

APPENDIX

In this Appendix the derivation of the semiclassical path representations for the time-independent N-photon transition amplitudes of Eqs. (22)–(24) is outlined [25]. As for the case $N=0$ the derivation of the semiclassical path representation starting from Eq. (21) has already been worked out in detail elsewhere [1,2,24] we concentrate in the following on cases with $N \geq 1$. The relevant N-photon transition amplitudes are then defined by Eqs. (19) and (20).

First, we describe the solution of the inhomogeneous Schrödinger equations (20). Using the notation of Sec. II and adopting the channel expansion [2]

$$\langle X,r|\lambda(\dots)\rangle = \sum_{j=1}^{3} \langle X|\Phi_j\rangle\langle r|F^{(j)}(r;\dots)\rangle/r \quad \text{(A1)}$$

they can be rewritten in the form (with $\varepsilon_1,\dots,\varepsilon_{N+1}$ arbitrary complex)

$$\{\varepsilon_1-[\mathbf{h}+\widetilde{\boldsymbol{\varepsilon}}_c+\widetilde{\mathbf{V}}(r)]\}\widetilde{\mathbf{F}}(r;\varepsilon_1)=\widetilde{\mathbf{D}}_g(r), \quad \text{(A2)}$$

$$\{\varepsilon_n-[\mathbf{h}+\widetilde{\boldsymbol{\varepsilon}}_c+\widetilde{\mathbf{V}}(r)]\}\widetilde{\mathbf{F}}(r;\varepsilon_n,\dots,\varepsilon_1)$$
$$=\widetilde{\mathbf{L}}\widetilde{\mathbf{F}}(r;\varepsilon_{n-1},\dots,\varepsilon_1) \quad (N \geq n \geq 2) \quad \text{(A3)}$$

and

$$\{\varepsilon_{N+1}-[\mathbf{h}+\widetilde{\boldsymbol{\varepsilon}}_c+\widetilde{\mathbf{V}}(r)]\}\overline{\widetilde{\mathbf{F}}}^*(r;\varepsilon_{N+1})=\widetilde{\mathbf{D}}_f^*(r). \quad \text{(A4)}$$

The channel coordinates X represent all coordinates of the core electrons and the angular momentum and spin of the excited Rydberg electron [17]. The radial-dependent column vectors $\widetilde{\mathbf{F}}(r;\varepsilon_1)$, $\widetilde{\mathbf{F}}(r;\varepsilon_n,\dots,\varepsilon_1)$, and $\overline{\widetilde{\mathbf{F}}}(r;\varepsilon_{N+1})$ are formed by the components of the states $|\lambda(\varepsilon_1)\rangle$, $|\lambda(\varepsilon_n,\dots,\varepsilon_1)\rangle$, and $|\overline{\lambda}(\varepsilon_{N+1})\rangle$ in the photon-dressed core channels whose relation to the bare core channels is defined by Eq. (25). The square matrix $\widetilde{\mathbf{V}}(r)=\mathbf{O}^T\mathbf{V}(r)\mathbf{O}$ describes the correlation-induced coupling between the photon-dressed core states which takes place at distances $r \lesssim r_c$ inside the ionic core. Thereby r_c denotes the core radius which has a typical value of a few Bohr radii. It is assumed that the angular momentum of the Rydberg electron is not changed by a radiative transition of the core [2]. Therefore the diagonal square matrix $\mathbf{h}$ commutes with the orthogonal (nonunitary) matrix $\mathbf{O}$. The radial-dependent column vectors $\widetilde{\mathbf{D}}_k(r)=\mathbf{O}^T\mathbf{D}_k(r)$ $(k=g,f)$ with components $(\mathbf{D}_g)_j(r)=r\int dX\Phi_j^*(X)\mathbf{d}\cdot\mathbf{e}_1\langle X,r|g\rangle$ and $(\mathbf{D}_f)_j(r)$ $=r\int dX\Phi_j^*(X)\mathbf{d}\cdot\mathbf{e}_2\langle X,r|f\rangle$ describe the initial excitation and final deexcitation of the Rydberg electron in the photon-dressed core channels.

In Eqs. (A2) and (A4) the terms on the right hand sides vanish approximately for $r \geq r_c$. The physical solutions of these inhomogeneous Schrödinger equations, which remain finite for both $r \to 0$ and $r \to \infty$, can be constructed as described in detail in Refs. [2,12,25]. For $r \geq r_c$ they are given by $\widetilde{\mathbf{F}}(r;\varepsilon_1)=\mathbf{C}(r;\varepsilon_1)\widetilde{\mathbf{V}}_1$ and $\overline{\widetilde{\mathbf{F}}}^*(r;\varepsilon_{N+1})=\mathbf{C}(r;\varepsilon_{N+1})\widetilde{\mathbf{U}}_{N+1}$ with

$$\widetilde{\mathbf{V}}_1=2\pi i(1-\widetilde{\chi}e^{2\pi i\widetilde{\boldsymbol{\nu}}_1})^{-1}\widetilde{\boldsymbol{\mathcal{D}}}_{g\mathbf{e}_1}^{(-)},$$

$$\widetilde{\mathbf{U}}_{N+1}=2\pi i(1-\widetilde{\chi}^T e^{2\pi i\widetilde{\boldsymbol{\nu}}_{N+1}})^{-1}\widetilde{\boldsymbol{\mathcal{D}}}_{f\mathbf{e}_2}^{(+)T}, \quad \text{(A5)}$$

and

$$\mathbf{C}(r;\varepsilon)=\tfrac{1}{2}[\boldsymbol{\Phi}^{(-)}(r;\varepsilon)e^{2\pi i\widetilde{\boldsymbol{\nu}}}-\boldsymbol{\Phi}^{(+)}(r;\varepsilon)]. \quad \text{(A6)}$$

Thereby, $\boldsymbol{\Phi}^{(\pm)}(r;\varepsilon)$ denote the diagonal matrices of (energy-normalized) incoming- and outgoing-wave Coulomb functions of complex energy ε (incorporating the thresholds $\widetilde{\boldsymbol{\varepsilon}}_c$), i.e., $[\boldsymbol{\Phi}^{(\pm)}(r;\varepsilon)]_{ii}=\phi^{(\pm)}(r;\varepsilon-\widetilde{\varepsilon}_{ci})$. Coulomb functions of complex energy are discussed in Ref. [29], for example. Except for ε lying on the branch cuts of $\widetilde{\boldsymbol{\nu}}$ (defined in the usual way) the functions $\mathbf{C}(r;\varepsilon)$ converge to zero for $r \to \infty$.

The column vectors of the (energy-normalized) photoionization and recombination dipole matrix elements are given by

$$\widetilde{\boldsymbol{\mathcal{D}}}_{g\mathbf{e}_1}^{(-)}=\int_0^\infty dr\widetilde{\boldsymbol{\mathcal{F}}}^{(-)\dagger}\widetilde{\mathbf{D}}_g, \quad \widetilde{\boldsymbol{\mathcal{D}}}_{f\mathbf{e}_2}^{(+)}=\int_0^\infty dr\widetilde{\mathbf{D}}_f^\dagger\widetilde{\boldsymbol{\mathcal{F}}}^{(+)}. \quad \text{(A7)}$$

Thereby the energy-normalized regular solutions of the homogeneous part of Eq. (A2) are defined by

$$\widetilde{\boldsymbol{\mathcal{F}}}^{(-)}(r;\varepsilon)=\tfrac{1}{2}[\boldsymbol{\Phi}^{(+)}(r;\varepsilon)-\boldsymbol{\Phi}^{(-)}(r;\varepsilon)\widetilde{\chi}^*] \quad \text{(A8)}$$

and $\widetilde{\boldsymbol{\mathcal{F}}}^{(+)}(r;\varepsilon)=-\widetilde{\boldsymbol{\mathcal{F}}}^{(-)}(r;\varepsilon)\widetilde{\chi}$.

The construction of the solutions of Eqs. (A3) for $r \geq r_c$ is complicated by the fact that the inhomogeneous term on the right hand side of Eq. (A3) is nonzero even at distances very

far from the ionic core. Nevertheless, this solution can be constructed by starting from the observation that for $r \geq r_c$ a particular solution of an equation of the form $\{\varepsilon_n - [\mathbf{h} + \widetilde{\boldsymbol{\varepsilon}}_c + \widetilde{\mathbf{V}}(r)]\}\widetilde{\mathbf{G}}(r;\varepsilon_n) = \mathbf{M}\mathbf{C}(r;\varepsilon_m)$ with an arbitrary matrix $\mathbf{M}$ and $\mathbf{C}(r;\varepsilon_m)$ defined by Eq. (A6) is given by $[\mathbf{M}]_{nm}\mathbf{C}(r;\varepsilon_m)$. Thereby, the matrix elements (ij) of $[\mathbf{M}]_{nm}$ are defined by

$$([\mathbf{M}]_{nm})_{ij} = \mathbf{M}_{ij}(\varepsilon_n - \widetilde{\varepsilon}_{ci} - \varepsilon_m + \widetilde{\varepsilon}_{cj})^{-1}. \quad (A9)$$

Thus by induction it follows that for $r \geq r_c$ a solution of Eq. (A3) which remains finite at least for $r \to \infty$ is given by

$$\widetilde{\mathbf{F}}(r;\varepsilon_n, \ldots, \varepsilon_1) = \sum_{k=1}^{n} \{\widetilde{\mathbf{L}}\}_{nk}\mathbf{C}(r;\epsilon_k)\widetilde{\mathbf{V}}_k. \quad (A10)$$

Thereby, the matrices $\{\widetilde{\mathbf{L}}\}_{nk}$ are defined recursively in terms of the matrices $[\widetilde{\mathbf{L}}]_{jk}$ by the relations

$$\{\widetilde{\mathbf{L}}\}_{kk} = \mathbf{1},$$

$$\{\widetilde{\mathbf{L}}\}_{jk} = [\widetilde{\mathbf{L}}\{\widetilde{\mathbf{L}}\}_{j-1,k}]_{jk} \quad (j \geq k+1). \quad (A11)$$

The still unknown column vectors $\widetilde{\mathbf{V}}_k$ with $2 \leq k \leq n$ are determined uniquely by the requirement that $\widetilde{\mathbf{F}}(r;\varepsilon_n, \ldots, \varepsilon_1)$ has to remain finite also for $r \leq r_c$. This requirement can be imposed on $\widetilde{\mathbf{F}}(r;\varepsilon_n, \ldots, \varepsilon_1)$ by assuming that due to the long range of the inhomogeneous term on the right hand side of Eq. (A3) its influence can be neglected for $r \leq r_c$. Thus $\widetilde{\mathbf{F}}(r;\varepsilon_n, \ldots, \varepsilon_1)$ can only remain finite for $r \leq r_c$ if it is proportional to the regular solution of the homogeneous part of Eq. (A3) which is given by Eq. (A8). At $r = r_c$ this requirement implies the relation

$$\widetilde{\mathbf{V}}_k = (1 - \widetilde{\boldsymbol{\chi}}e^{2\pi i \widetilde{\nu}_k})^{-1} \sum_{k'=1}^{n-1} (\widetilde{\boldsymbol{\chi}}\{\widetilde{\mathbf{L}}\}_{kk'}e^{2\pi i \widetilde{\nu}_{k'}} - \{\widetilde{\mathbf{L}}\}_{kk'})\widetilde{\mathbf{V}}_{k'} \quad (A12)$$

for $n \geq k \geq 2$. This equation can be solved recursively for $k \geq 2$ starting with $\widetilde{\mathbf{V}}_1$ as given by Eq. (A5).

From the knowledge of the behavior of the solutions of the inhomogeneous Schrödinger equations for $r \geq r_c$ and arbitrary values of the photon number N the matrix element of Eq. (19) can be evaluated. Thereby it is assumed that the dominant contribution to this matrix element comes from distances $r \geq r_c$ outside the core region. This assumption is justified as long as the states involved in the matrix element of Eq. (19) extend over distances which are large in comparison with the core radius r_c because in this case the neglected contribution is expected to be small. Thus, using the known relation for matrix elements of radial Coulomb functions [30,31], i.e.,

$$\int_{r_c}^{\infty} dr \mathbf{C}(r;\varepsilon_2)\mathbf{M}\mathbf{C}(r;\varepsilon_1)$$

$$= \frac{1}{2\pi i}([\mathbf{M}]_{21}e^{2\pi i \nu_1} - e^{2\pi i \nu_2}[\mathbf{M}]_{21}), \quad (A13)$$

with $\mathbf{M}$ denoting an arbitrary square matrix and $\mathbf{C}(r;\varepsilon)$ the Coulomb functions of Eq. (A6), one obtains the result

$$T_{g \to f}^{(1)}(\varepsilon_2,\varepsilon_1) = 2\pi i \widetilde{\boldsymbol{\mathcal{D}}}_{f\mathbf{e}_2}^{(+)}(e^{-2\pi i \widetilde{\nu}_2} - \widetilde{\boldsymbol{\chi}})^{-1}$$

$$\times \widetilde{\mathbf{W}}_{2,1}(e^{-2\pi i \widetilde{\nu}_1} - \widetilde{\boldsymbol{\chi}})^{-1}\widetilde{\boldsymbol{\mathcal{D}}}_{g\mathbf{e}_1}^{(-)},$$

$$T_{g \to f}^{(N)}(\varepsilon_{N+1}, \ldots, \varepsilon_1) = 2\pi i \widetilde{\boldsymbol{\mathcal{D}}}_{f\mathbf{e}_2}^{(+)}(e^{-2\pi i \widetilde{\nu}_{N+1}} - \widetilde{\boldsymbol{\chi}})^{-1}$$

$$\times \Bigg(\sum_{(k_p, \ldots, k_1)} \widetilde{\mathbf{W}}_{N+1,k_p}$$

$$\times (e^{-2\pi i \widetilde{\nu}_{k_p}} - \widetilde{\boldsymbol{\chi}})^{-1}$$

$$\times \widetilde{\mathbf{W}}_{k_p, k_{p-1}} \cdots$$

$$\times (e^{-2\pi i \widetilde{\nu}_{k_2}} - \widetilde{\boldsymbol{\chi}})^{-1}\widetilde{\mathbf{W}}_{k_2,k_1}$$

$$\times (e^{-2\pi i \widetilde{\nu}_{k_1}} - \widetilde{\boldsymbol{\chi}})^{-1}\widetilde{\mathbf{W}}_{k_1,1} \Bigg)$$

$$\times (e^{-2\pi i \widetilde{\nu}_1} - \widetilde{\boldsymbol{\chi}})^{-1}\widetilde{\boldsymbol{\mathcal{D}}}_{g\mathbf{e}_1}^{(-)} \quad (N \geq 2). \quad (A14)$$

Thereby, the matrices $\widetilde{\mathbf{W}}_{m,n}$ are given by

$$\widetilde{\mathbf{W}}_{m,n} = \sum_{l=n}^{m} (-1)^{n-l+1}\{\widetilde{\mathbf{L}}\}_{m,l}e^{-2i\pi\widetilde{\nu}_l}\langle\widetilde{\mathbf{L}}\rangle^{ln}, \quad (A15)$$

with $1 \leq n \leq m-1$ and the matrices $\langle\widetilde{\mathbf{L}}\rangle^{ln}$ being defined recursively in terms of the matrices $[\widetilde{\mathbf{L}}]_{jk}$ by

$$\langle\widetilde{\mathbf{L}}\rangle^{kk} = \mathbf{1},$$

$$\langle\widetilde{\mathbf{L}}\rangle^{jk} = [\langle\widetilde{\mathbf{L}}\rangle^{j,k+1}\widetilde{\mathbf{L}}]_{jk} \quad (j \geq k+1). \quad (A16)$$

The matrices $\langle\widetilde{\mathbf{L}}\rangle^{jk}$ and $\{\widetilde{\mathbf{L}}\}_{lm}$ are related via

$$\sum_{k=1}^{n} (-1)^k \{\widetilde{\mathbf{L}}\}_{nk}\langle\widetilde{\mathbf{L}}\rangle^{k1} = \sum_{k=1}^{n} (-1)^k \langle\widetilde{\mathbf{L}}\rangle^{nk}\{\widetilde{\mathbf{L}}\}_{k1} = \mathbf{0}.$$

For $N \geq 2$ the sum in Eq. (A14) extends over all possible p-tuples of integers $(k_p, k_{p-1}, \ldots, k_1)$ with $N-1 \geq p \geq 1$, $N \geq k_p > k_{p-1} > \cdots > k_1 \geq 2$, and $\{k_p, \ldots, k_1\}$ being one of the possible subsets of the set of numbers $\{N, \ldots, 2\}$ and over the empty set which corresponds to the term containing $\widetilde{\mathbf{W}}_{N+1,1}$ only.

It can be shown that the N-photon amplitudes as given by Eqs. (A14) are as a function of each ε_k analytic on the whole complex plane, except for poles and branch cuts, the locations of which are determined by those of the function $\det(e^{-2\pi i \widetilde{\nu}} - \widetilde{\boldsymbol{\chi}})$. In particular, this implies that the singularities which seem to be introduced by the matrices $\widetilde{\mathbf{W}}_{m,n}$ are removable. Furthermore, the expressions (A14) remain bounded, i.e., do not become exponentially large, if one or several ε_k approach a branch cut. This observation justifies the calculation of bounded wave packet dynamics only with residue contributions as it was mentioned at the end of Sec. II B.

The expressions (A14) for the N-photon amplitudes are valid on the whole complex (product) plane C^N apart from the singularities and branch cuts. The semiclassical path representation of Eqs. (A14), which is only valid in a region of the complex plane bounded from below by the branch cuts,

is derived by expanding the factors of the type $(1-\widetilde{\chi}e^{-2\pi i\widetilde{\nu}})^{-1}$ into geometric series and reorganizing the resulting sums, which finally leads to Eqs. (23) and (24) [25]. The exact definition of the matrices $\widetilde{\mathbf{S}}_{m,k}$ is given by

$$\widetilde{\mathbf{S}}_{m,k}=e^{2i\pi\widetilde{\nu}_m}\widetilde{\mathbf{I}}_{mk}(\tau=0),\qquad(\text{A}17)$$

with

$$\widetilde{\mathbf{I}}_{mk}(\tau)=\sum_{l=k}^{m}(-1)^{l-k}e^{-2i\pi\widetilde{\nu}_m}\{\widetilde{\mathbf{L}}\}_{ml}e^{2i\pi\widetilde{\nu}_l(1-\tau/T)}$$

$$\times\langle\widetilde{\mathbf{L}}\rangle^{lk}e^{2i\pi\widetilde{\nu}_k\tau/T}.\qquad(\text{A}18)$$

For the physical interpretation of the quantities $\widetilde{\mathbf{S}}_{m,k}$ it is convenient to rewrite Eq. (A18) as a recursive integral equation

$$\widetilde{\mathbf{I}}_{mk}(\tau)=\int_{\tau}^{T}d\tau_k\widetilde{\mathbf{I}}_{m,k+1}(\tau_k)e^{-2i\pi\widetilde{\nu}_{k+1}\tau_k/T}(e^{-i\pi/2}\widetilde{L})$$

$$\times e^{2i\pi\widetilde{\nu}_k\tau_k/T}\quad(1\leq k<m),\qquad(\text{A}19)$$

which is valid under the approximation that the relation between energy and effective quantum numbers $\widetilde{\nu}_j$ is approximately linear, i.e.,

$$[\varepsilon_l-\widetilde{\varepsilon}_{cj}-(\varepsilon_k-\widetilde{\varepsilon}_{ci})]^{-1}\simeq\frac{T}{2\pi[(\widetilde{\nu}_l)_{jj}-(\widetilde{\nu}_k)_{ii}]}.\quad(\text{A}20)$$

Solving Eq. (A19) iteratively Eq. (28) of Sec. II B is obtained. When performing the Laplace transform the linear approximation in Eq. (A20) has to be applied at those energies which contribute the most for given t_b-t_a and M_i leading to the determination of T mentioned in Sec. II.

---

[1] G. Alber and P. Zoller, Phys. Rep. **199**, 231 (1991).

[2] O. Zobay and G. Alber, Phys. Rev. A **52**, 541 (1995).

[3] L. G. Hanson and P. Lambropoulos, Phys. Rev. Lett. **74**, 5009 (1995).

[4] W. E. Cooke, T. F. Gallagher, S. A. Edelstein, and R. M. Hill, Phys. Rev. Lett. **40**, 178 (1978).

[5] T. F. Gallagher, *Rydberg Atoms* (Cambridge University Press, Cambridge, England, 1994).

[6] X. Wang and W. E. Cooke, Phys. Rev. Lett. **67**, 976 (1991); Phys. Rev. A **46**, R2201 (1992); **46**, 4347 (1992).

[7] J. G. Story, D. I. Duncan, and T. F. Gallagher, Phys. Rev. Lett. **71**, 3431 (1993).

[8] R. R. Jones and P. H. Bucksbaum, Phys. Rev. Lett. **67**, 3215 (1991).

[9] H. Stapelfeldt, D. G. Papaioannou, L. D. Noordam, and T. F. Gallagher, Phys. Rev. Lett. **67**, 3223 (1991).

[10] B. Walker, M. Kaluza, B. Sheehy, P. Agostini, and L. F. Di-Mauro, Phys. Rev. Lett. **75**, 633 (1995).

[11] N. J. van Druten and H. G. Muller, J. Phys. B **29**, 15 (1996).

[12] F. Robicheaux, Phys. Rev. A **47**, 1391 (1993).

[13] L. G. Hanson, J. Zhang, and P. Lambropoulos, Europhys. Lett. **30**, 81 (1995).

[14] S. L. Haan, M. Bolt, H. Nymeyer, and R. Grobe, Phys. Rev. A **51**, 4640 (1995).

[15] N. J. van Druten and H. G. Muller, Phys. Rev. A **52**, 3047 (1995).

[16] B. R. Mollow, Phys. Rev. A **12**, 1919 (1975).

[17] M. J. Seaton, Rep. Prog. Phys. **46**, 167 (1983).

[18] J. Dalibard, Y. Castin, and K. Mølmer, Phys. Rev. Lett. **68**, 580 (1992).

[19] R. Dum, A. S. Parkins, P. Zoller, and C. W. Gardiner, Phys. Rev. A **46**, 4382 (1992).

[20] H. J. Carmichael, *An Open Systems Approach to Quantum Optics* (Springer-Verlag, Berlin, 1993).

[21] U. Fano and A. R. P. Rau, *Atomic Collisions and Spectra* (Academic Press, New York, 1986).

[22] H. H. Fielding, J. Phys. B **27**, 5883 (1994).

[23] G. Alber, H. Ritsch, and P. Zoller, Phys. Rev. A **34**, 1058 (1986).

[24] G. Alber and P. Zoller, Phys. Rev. A **37**, 377 (1988).

[25] O. Zobay, Ph.D. thesis, Universität Freiburg im Breisgau, 1996.

[26] G. M. Lankhuijzen and L. D. Noordam, Phys. Rev. Lett. **76**, 1784 (1996).

[27] P. Lambropoulos and P. Zoller, Phys. Rev. A **24**, 379 (1981).

[28] L. G. Hanson, Masters thesis, University of Copenhagen, 1995.

[29] M. J. Seaton, Mon. Not. R. Astron. Soc. **118**, 504 (1958).

[30] S. A. Bhatti, C. L. Cromer, and W. E. Cooke, Phys. Rev. A **24**, 161 (1981).

[31] R. H. Bell and M. J. Seaton, J. Phys. B **18**, 1589 (1985).